Available online at www.sciencedirect.com

ScienceDirect

Advances in Space Research xxx (xxxx) xxx

ADVANCES IN SPACE RESEARCH (a COSPAR publication)

www.elsevier.com/locate/asr

Innovative Systems Engineering Solutions for Power-Positive Operations: Navigating the Multi-Constraint Challenges of the SWARM-EX CubeSat Mission

David J. Fitzpatrick *, Scott E. Palo

Ann and H.J. Smead Department of Aerospace Engineering Sciences, University of Colorado, Boulder, 3775 Discovery Drive, Boulder, CO 80303, USA

Received 7 November 2023; received in revised form 20 May 2024; accepted 21 June 2024

Abstract

Although the small stature of CubeSats and their standardized deployer options help to lower unit development cost and facilitate launch opportunities, the physical size limits of CubeSats prove to be a double-edged sword vis-à-vis sustaining a stable power state while hosting instruments with high power demands and often strict pointing requirements. For the Space Weather Atmospheric Reconfigurable Multiscale-EXperiment (SWARM-EX), this issue is magnified by the mission's ambitious goals; to comply with mission requirements, a SWARM-EX spacecraft is required to concurrently (1) point the science instruments no more than 30° off ram when they are operational, (2) point the GPS patch antenna no more than 30° off zenith at least once per orbit, (3) point the boresight of the X-Band patch antenna no more than 18° from the ground station during downlink, (4) maximize the differential cross-sectional area during differential drag maneuvers, and (5) maximize solar array power generation at all times. Consequently, leading-edge CubeSat missions like SWARM-EX require innovative systems engineering solutions to remain power-positive during on-orbit operations. Through the design of a comprehensive module-based concept of operations, orbital power generation simulations, intricate constrained attitude profiles, and a configurable battery state of charge simulation tool, the SWARM-EX mission designers have conceived a plan to retire the risk of not maintaining a power-positive state while successfully meeting all mission requirements; it is the aim of the authors to illuminate these strategies as a case study.

Keywords: CubeSat; Small satellites; Systems engineering; Constrained attitude profiles; Power budget; SWARM-EX

1. Introduction

Ever since the term was publicly coined out of the California Polytechnic State University in 2000, the standardized picosatellite known as the "CubeSat" has served as an ideal agent for educational engagement in the satellite development domain (Puig-Suari et al., 2001). CubeSats (small, standardized, rectangular satellites with masses below 14 [kg]) are constructed to be compatible with standardized deployer and launch interfaces, and the miniaturization and standardization afforded by their design has allowed them to flourish in both academic and professional aerospace communities. In a contemporary space era spawned from the reusable rockets and large satellite constellations of industry leaders, academic institutions like the University of Colorado (CU) Boulder have exhibited the ability of CubeSats such as CSSWE (Li et al., 2013), QB50 Challenger (Palo et al., 2015), MinXSS (Woods et al., 2016), and others to transcend mere instruments of teaching, leveraging them for remarkable space missions capable of making significant advances to both scientific and technological fields. In the wake of the success of these

* Corresponding author.
E-mail addresses: david.fitzpatrick@colorado.edu (D.J. Fitzpatrick), scott.palo@colorado.edu (S.E. Palo).

https://doi.org/10.1016/j.asr.2024.06.057
0273-1177/

Please cite this article as: D. J. Fitzpatrick and S. E. Palo, Innovative Systems Engineering Solutions for Power-Positive Operations: Navigating the Multi-Constraint Challenges of the SWARM-EX CubeSat Mission, Advances in Space Research, https://doi.org/10.1016/j.asr.2024.06.057

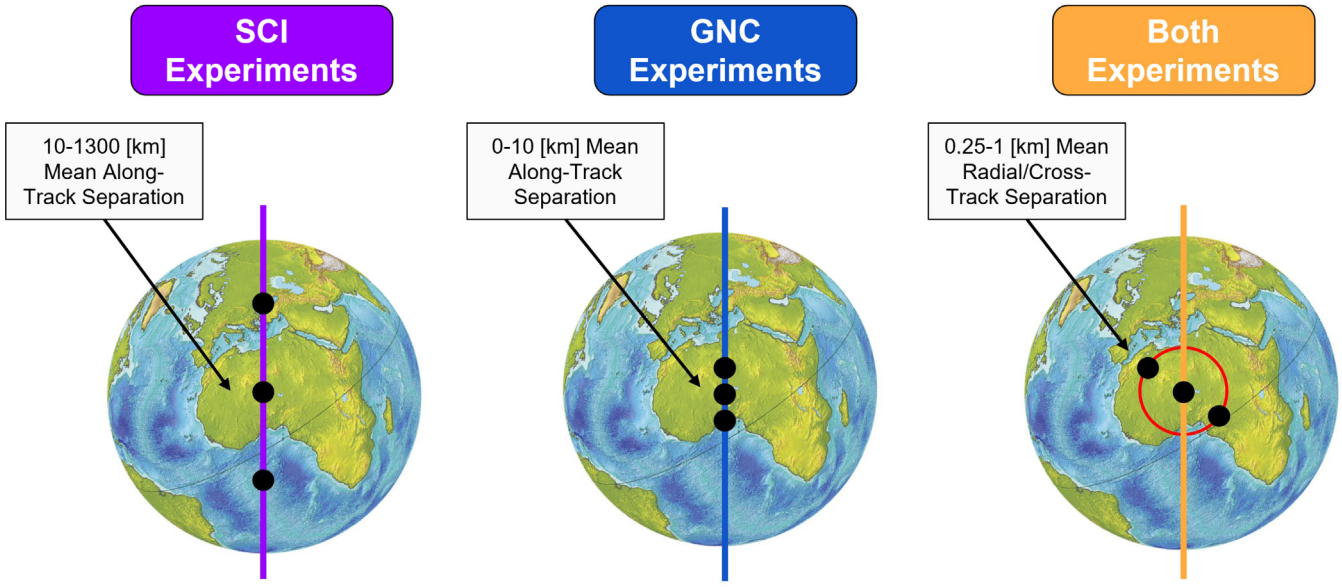

Fig. 1. A visual representation of SWARM-EX's SCI and GNC experiments detailing their differing ranges of mean along-track separation and string-of-pearls formation.

missions, one of CU Boulder's newest and most promising CubeSat missions is the National Science Foundation (NSF)-funded Space Weather Atmospheric Reconfigurable Multiscale-EXperiment (SWARM-EX), an inter-collegiate CubeSat initiative to launch three identical CubeSats in a reconfigurable "swarm" into Low-Earth Orbit (LEO) (Lowe et al., 2024).

With a nominal launch date in Q1 2026, SWARM-EX is a collaboration between CU Boulder, Stanford University, Georgia Institute of Technology, Western Michigan University, University of Southern Alabama, and Olin College. The primary objectives of the mission are twofold: (1) to better characterize the spatial and temporal variability of the Equatorial Ionization Anomaly (EIA; Appleton (1946)) and the Equatorial Thermospheric Anomaly (ETA; Liu et al. (2007)); and (2) to advance the state of the art in autonomous formation flying through a novel hybrid propulsive/differential-drag control methodology (Hunter and D'Amico, 2022). Flying in a string-of-pearls formation, the SWARM-EX CubeSats will address these objectives by alternating between conducting Science (SCI) experiments and Guidance, Navigation, & Control (GNC) experiments, where the former are characterized by much larger mean along-track separations between the spacecraft than the latter (Fig. 1).[1] Each CubeSat will be equipped with a low-rate Ultra-High Frequency (UHF) radio, a high-rate X-Band radio (downlink only), a scalable cold-gas propulsion system, and a high-performance Attitude Determination & Control System (ADCS) to demonstrate the key technologies of on-board autonomy, inter-satellite links, propulsion, and multiuser communications. A Flux-Probe EXperiment (FIPEX; Eberhart et al. (2015)) neutral oxygen sensor and Langmuir Probe (LP; Fish et al. (2014)) measuring ion density will also be onboard to address outstanding questions in aeronomy relevant to the EIA/ETA. During SCI experiments, the three CubeSats of SWARM-EX will separate from one another using a combination of onboard propulsion and differential drag to make in situ measurements of atomic oxygen, the dominant atmospheric component in LEO and the key to better understanding the EIA and ETA. The spacecraft are then brought much closer together during GNC experiments, where they will further demonstrate fuel balancing through the hybrid control scheme and precise relative orbit determination and prediction. A mean along-track separation of $\approx$10 [km] nominally partitions these two experiments.

Although the small stature of CubeSats and their standardized deployer options help to lower unit development cost and facilitate launch opportunities, the physical size limits of CubeSats prove to be a double-edged sword vis-à-vis sustaining a stable power state while hosting instruments with high power demands and often strict pointing requirements. For SWARM-EX, this issue is magnified by the mission's ambitious goals; to comply with mission requirements, a SWARM-EX spacecraft is required to concurrently adhere to numerous attitude requirements (Fig. 2), including:

1. Point the science instruments no more than 30° off ram (the direction of spacecraft motion) when they are operational;
2. Point the Global Positioning System (GPS) patch antenna no more than 30° off zenith (the direction normal to the surface of the Earth) at least once per orbit;

[1] Both experiments require nonzero mean radial/cross-track separation distances between spacecraft in an effort to considerably mitigate the risk of conjunctions within the swarm.

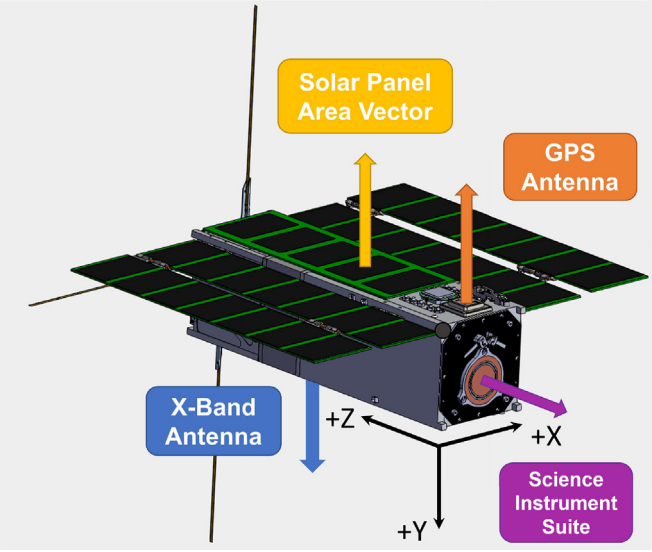

Fig. 2. A rendering of a SWARM-EX CubeSat detailing the science instrument suite, GPS patch antenna, X-Band patch antenna, and solar panel area pointing vectors alongside the spacecraft body axes.

3. Point the boresight (the axis of maximum antenna gain) of the X-Band patch antenna no more than 18° from the ground station during downlink;
4. Maximize the differential cross-sectional area between the spacecraft during differential drag maneuvers; and
5. Maximize solar array power generation at all times.

The attitude requirements imposed by the onboard systems engenders complex challenges for the SWARM-EX mission designers, particularly with regards to ensuring that all spacecraft remain "power-positive" during on-orbit operations (i.e., the spacecraft are able to generate at least as much power as they expend). For a given spacecraft to sustain a stable power state throughout an orbit, power draw must be balanced by power generation through appropriately sized and oriented spacecraft solar panels. The layout, size, and general design of the solar panels must meet the system's needs while accounting for eclipses and panel orientation throughout the orbit, including instances where pointing requirements force the solar panels to deviate from the Sun. While certain small satellites, such as those comprising SpaceX's Starlink constellation, benefit from orientable solar arrays facilitated by sophisticated mechanisms such as solar array drive assemblies, others, like the SWARM-EX CubeSat, forego this additional degree of freedom due to the associated complexities and cost implications. In such cases, ensuring a stable power cycle becomes imperative within the confines of the constraints of the mission, particularly when the orientation of the solar panels remains static relative to the spacecraft bus, tightly coupling their alignment with other critical pointing vectors. Leading-edge CubeSat missions such as SWARM-EX therefore require a carefully-crafted operations plan driven by a comprehensive power analysis to realize the mission's core objectives. While previous studies, such as those by Marshall et al. (2020) and Porras-Hermoso et al. (2024), have pursued formalized multi-objective optimization strategies aimed at minimizing a cost function to achieve power-optimal tracking, this research presents an alternative approach. Here, a geometrically derived constrained attitude profile, capable of concurrently satisfying the diverse pointing requirements inherent to the mission, is proposed in the context of the mission's Concept of Operations (ConOps).

This paper presents a discussion of the innovative systems engineering solutions taken by the SWARM-EX mission designers to retire the risk of not maintaining a power-positive state while successfully meeting all mission requirements. Section 2 begins with a discussion of the module-based paradigm for the ConOps on which the subsequent power analysis for SWARM-EX is founded. Section 3 then provides an introduction to performing a power analysis for a satellite mission and presents an overview of the SWARM-EX solar array design and orbital parameters. Next, Section 4 details the derivation of the constrained attitude profiles for SCI experiments and their profound improvement to power generation. The implications such attitude profiles have on the usage of differential drag in the mission is described in Section 4.4. Section 4.5 then completes the power discussion by presenting a configurable battery State of Charge (SoC) simulation tool built in Microsoft Excel. Finally, Section 5 offers concluding remarks and postulates extensions of the established approach to other small satellite missions.

2. SWARM-EX Operational Modes and Orbital Timelines

Due to the many pointing constraints and high-power demands of the science instrument suite, the SWARM-EX mission designers have identified the risk of not maintaining a power-positive state throughout its lifetime as being especially relevant. To address this concern, SWARM-EX mission designers have developed a module-based ConOps that is able to characterize all of the combinations of active onboard hardware that are expected on-orbit to distinguish each associated power-draw state. This paradigm is comprised of two types of modules: (1) unique combinations of operational onboard hardware (i.e., reaction wheels, radiating antennas, science instrumentation, propulsion, etc.) known as "operational modes," and (2) unique combinations of operational modes appropriately sequenced at varying duty cycles over the course of a single orbit known as "orbital timelines."

The SWARM-EX mission designers have developed twenty-one operational modes in which the spacecraft will function. As detailed in Fig. 3, three of these operational modes are related to the FIPEX when in use: `FPX1`, `FPX2`, and `FPX3`. `FPX1` serves as the foundation for FIPEX operations and is characterized by power draw from the FIPEX, LP, GPS radio, UHF radio (receive only), and core avionic systems such as the Electrical Power System (EPS), Command & Data Handling

Components	Voltage Line [V]	Mature Power [W]	FPX1	FPX2	FPX3
EPS Board	3.3	0.3	0.3	0.3	0.3
CDH Board		0.2	0.2	0.2	0.2
GNC Processor		1.6	1.6	1.6	1.6
GPS		2.0	2.0	2.0	2.0
PROP Electronics + Sensors		0.2	0.2	0.2	0.2
ADCS	12	5.6	5.6	5.6	5.6
ADCS Peak Power		9.5			
UHF Radio (RX)	12	1.6	1.6	1.6	1.6
UHF Radio (TX)		15.5		15.5	15.5
FIPEX	24	1.7	1.7	1.7	1.7
FIPEX Sensor		4.5	4.5	4.5	4.5
Langmuir Probe	10.9	1.5	1.5	1.5	1.5
X-Band Radio		15.8			15.8
PROP Misc. Electronics		0.0	0.0	0.0	0.0
PROP Valves		8.4			
Battery Heaters		13.0			
Power Totals [W]:			19.2	34.7	50.4

Fig. 3. The FPX1, FPX2, and FPX3 operational modes alongside their power draws and associated voltage lines for the SWARM-EX mission.

(CDH), GNC, and propulsion (PROP) microcontrollers. With this baseline established, FPX2 is defined as being identical to FPX1 except with the UHF radio transmitting. This distinction necessitates the creation of a separate operational mode due to the difference in power draw from the UHF radio. Likewise, FPX3 is identical to FPX2 except with the X-Band radio transmitting as well. Constructing all operational modes which are realistic[2] for SWARM-EX allows designers to identify portions of the mission where power usage is especially high and, more generally, prepare for the entire mission in terms of power.

These twenty-one operational modes serve as the building blocks for fifteen orbital timelines which fully capture the operations of SWARM-EX. These timelines have been identified such that at any given point within the lifetime of the mission, the spacecraft of SWARM-EX will be operating in one of these fifteen timelines. As illustrated in Fig. 4, there are four timelines related to SCI experiments, two timelines related to GNC experiments, two timelines related to differential drag experiments, five timelines related to commissioning, a Safe Mode timeline, and a Phoenix Mode timeline.[3] Each orbital timeline is comprised of a unique sequence of operational modes that vary in duration as a fraction of a percent of an orbit (i.e., duty-cycling), where the summation of the duty cycles of all operational modes within a timeline is always 100%. Each timeline is also specific to the SWARM-EX mission. For example, given that the EIA/ETA are equatorial phenomena, the total operational time for the science instruments (both the FIPEX and LP) is set at 43% of a SCI orbit to yield the desired latitudinal coverage, where that fraction is centered about the equator. Moreover, the time during which a SWARM-EX spacecraft will be visible to a ground-station receiver (UHF or X-Band) has been estimated at ≈6% of an orbit, yielding a 6% duty cycle for modes like FPX2, FPX3, GS OPS, SP5, and others specific to radio downlink periods.[4]

This modular approach of piecing operational modes into orbital timelines provides a comprehensive understanding of the onboard power usage for the SWARM-EX mission. When linked with the subsequent orbital power generation simulation delineated in subsequent sections, this approach allows for full characterization of the spacecraft power state and associated battery SoC.

3. Introduction to Orbital Power Generation Simulation and Constrained Attitude Profiles

While a module-based ConOps systematically evaluates onboard power usage, this power draw analysis must be paired with a comparable study of the power generated by each spacecraft on-orbit to affirm a power-positive state

[2] Although the 16 hardware components (each with unique power draws) of Fig. 3 can technically be ordered in 16! ≈ 2.1×10^{13} ways, many of these combinations are not realistic for on-orbit operations. As a result, most theoretical combinations are ignored, and the total number of operational modes considered is far less than the total possible number of combinations.

[3] Phoenix Mode can be thought of as an "ultra-Safe" mode, where only the CDH, EPS, and the UHF receiver are operational, and the spacecraft is without attitude control (i.e., "tumbling").

[4] The distinction between the ground station being on the dayside vs. the nightside is based on the fact that the FIPEX only takes valuable measurements on the dayside. Likewise, the distinction between "w/" and "w/o" X-Band is due to the lack of need for downlink on the X-Band every orbit.

Operational Orbits Summary

	SCI Orbit w/ X-Band: Ground Station is Dayside				SCI Orbit w/o X-Band: Ground Station is Dayside				SCI Orbit w/ X-Band: Ground Station is Nightside			
	Name	Draw [W]	Duty Cycle	Weighted [W]	Name	Draw [W]	Duty Cycle	Weighted [W]	Name	Draw [W]	Duty Cycle	Weighted [W]
Mode 1:	FPX1	19.2	24%	4.6	FPX1	19.2	24%	4.6	FPX1	19.2	29%	5.6
Mode 2:	FPX3	50.4	6%	3.0	FPX2	34.7	6%	2.1	PROP SCI	27.6	1%	0.3
Mode 3:	FPX1	19.2	13%	2.5	FPX1	19.2	13%	2.5	FPX1	19.2	13%	2.5
Mode 4:	SP1	11.6	56%	6.5	SP1	11.6	56%	6.5	SP1	11.6	37%	4.3
Mode 5:	PROP	20.0	1%	0.2	PROP	20.0	1%	0.2	GS OPS	42.8	6%	2.6
Mode 6:									SP1	11.6	14%	1.6
Energy / Power Summary	Average Energy [Wh]:		Average Power [W]:		Average Energy [Wh]:		Average Power [W]:		Average Energy [Wh]:		Average Power [W]:	
Draw:	26.1		16.8		24.6		15.9		26.1		16.8	

	SCI Orbit w/o X-Band: Ground Station is Nightside				GNC Orbit w/ X-Band				GNC Orbit w/o X-Band			
	Name	Draw [W]	Duty Cycle	Weighted [W]	Name	Draw [W]	Duty Cycle	Weighted [W]	Name	Draw [W]	Duty Cycle	Weighted [W]
Mode 1:	FPX1	19.2	29%	5.6	SP1	11.6	23%	2.7	SP1	11.6	23%	2.7
Mode 2:	PROP SCI	27.6	1%	0.3	PROP	20.0	1%	0.2	PROP	20.0	1%	0.2
Mode 3:	FPX1	19.2	13%	2.5	GS OPS	42.8	6%	2.6	SP5	27.0	6%	1.6
Mode 4:	SP1	11.6	37%	4.3	SP1	11.6	70%	8.1	SP1	11.6	70%	8.1
Mode 5:	SP5	27.0	6%	1.6								
Mode 6:	SP1	11.6	14%	1.6								
Energy / Power Summary	Average Energy [Wh]:		Average Power [W]:		Average Energy Draw [Wh]:		Average Power Draw [W]:		Average Energy Draw [Wh]:		Average Power Draw [W]:	
Draw:	24.6		15.9		21.0		13.5		19.5		12.6	

	Safe Mode Orbit				Phoenix Mode Orbit				UHF Commissioning Orbit			
	Name	Draw [W]	Duty Cycle	Weighted [W]	Name	Draw [W]	Duty Cycle	Weighted [W]	Name	Draw [W]	Duty Cycle	Weighted [W]
Mode 1:	SAFE	11.3	20%	2.3	PHX	2.1	100%	2.1	UHF CM1	5.7	20%	1.1
Mode 2:	SP5	27.0	6%	1.6					UHF CM2	21.2	6%	1.3
Mode 3:	SAFE	11.3	74%	8.4					UHF CM1	5.7	74%	4.2
Energy / Power Summary	Average Energy Draw [Wh]:		Average Power Draw [W]:		Average Energy Draw [Wh]:		Average Power Draw [W]:		Average Energy Draw [Wh]:		Average Power Draw [W]:	
Draw:	19.0		12.3		3.3		2.1		10.3		6.6	

	X-Band Commissioning Orbit				Propulsion Commissioning Orbit w/ X-Band				Propulsion Commissioning Orbit w/o X-Band			
	Name	Draw [W]	Duty Cycle	Weighted [W]	Name	Draw [W]	Duty Cycle	Weighted [W]	Name	Draw [W]	Duty Cycle	Weighted [W]
Mode 1:	ADCS CM1	11.3	20%	2.3	SAFE	11.3	20%	2.3	SAFE	11.3	20%	2.3
Mode 2:	GS XCM	42.5	6%	2.6	GS OPS	42.8	6%	2.6	SP5	27.0	6%	1.6
Mode 3:	ADCS CM1	11.3	74%	8.4	PROP SCI	27.6	1%	0.3	PROP SCI	27.6	1%	0.3
Mode 4:					SAFE	11.3	73%	8.3	SAFE	11.3	73%	8.3
Energy / Power Summary	Average Energy Draw [Wh]:		Average Power Draw [W]:		Average Energy Draw [Wh]:		Average Power Draw [W]:		Average Energy Draw [Wh]:		Average Power Draw [W]:	
Draw:	20.5		13.2		20.7		13.4		19.3		12.4	

	ADCS Commissioning Orbit				Low Drag w/ X-Band				Low Drag w/o X-Band			
	Name	Draw [W]	Duty Cycle	Weighted [W]	Name	Draw [W]	Duty Cycle	Weighted [W]	Name	Draw [W]	Duty Cycle	Weighted [W]
Mode 1:	ADCS CM1	11.3	20%	2.3	SP1	11.6	24%	2.8	SP1	11.6	24%	2.8
Mode 2:	ADCS CM2	26.8	6%	1.6	GS OPS	42.8	6%	2.6	SP5	27.0	6%	1.6
Mode 3:	ADCS CM1	11.3	74%	8.4	SP1	11.6	70%	8.1	SP1	11.6	70%	8.1
Energy / Power Summary	Average Energy Draw [Wh]:		Average Power Draw [W]:		Average Energy Draw [Wh]:		Average Power Draw [W]:		Average Energy Draw [Wh]:		Average Power Draw [W]:	
Draw:	19.0		12.2		20.9		13.5		19.4		12.5	

Fig. 4. The fifteen orbital timelines defined from the twenty-one operational modes for the SWARM-EX mission.

throughout the mission. For this reason, the SWARM-EX mission designers have conducted an analysis of the orbital power generation by the CubeSat swarm which couples custom pointing profiles and operational orbits with solar panel power generation.

The ability of a CubeSat to generate power through its solar panels is a common example of how the advantages arising from the standard's design simplicity can also manifest consequential shortcomings. While oftentimes more expensive satellite missions implement motorized hinge designs to adjust the angle of the solar panels without rotating the entire spacecraft, CubeSats like SWARM-EX have their solar panel direction vector static relative to the spacecraft body. As a result, tilting the solar panels towards the Sun requires a rotation of the entire spacecraft, which without careful consideration can easily result in the spacecraft violating a separate pointing constraint. For example, when SWARM-EX gathers data on the EIA and ETA through the FIPEX and the LP, both instruments require atomic oxygen flow in the anti-ram direction ($+\widehat{Z}$; Fig. 2). However, although pointing the instruments in the ram direction enables optimal measurements, this also regularly tilts the spacecraft solar panels away from the Sun, thereby resulting in a cosine power loss for power P defined by

$$P = \eta\vec{\mathcal{J}} \cdot \vec{A} = \eta\mathcal{J}A\cos\theta, \tag{1}$$

where η is the solar panel efficiency, $\vec{\mathcal{J}} = \mathcal{J}\widehat{S}$ is the solar panel flux vector parallel to the Sun unit vector $\widehat{S}$ originating at the spacecraft and pointing towards the Sun for solar constant $\mathcal{J} \approx 1361\ [\mathrm{W}\cdot\mathrm{m}^{-2}]$, $\vec{A}$ is the solar panel area vector, and θ is the angle between $\widehat{S}$ and $\vec{A}$.[5] This varying cosine loss, along with the high-power usage of the instrument suite ($\approx$8 [W] combined; Fig. 3), inhibits the SWARM-EX spacecraft from maintaining a stable power state in a fully ram-aligned attitude configuration (i.e., the ideal configuration for the science instruments).

In response, the SWARM-EX mission designers have developed a more complex attitude configuration to maximize solar panel power generation while still collecting valuable science data. Based on an empirical study, the SWARM-EX instrument team has determined that the angles off ram that yield the minimum allowable Signal-to-Noise-Ratio (SNR) are 30° and 45° for the FIPEX and the LP, respectively. Consequently, during SCI experiments, the SWARM-EX spacecraft constrain the instrument pointing vectors to a $\psi = 30°$ or $\lambda = 45°$-cone off ram while simultaneously maximizing the time spent with the solar panels normal to the Sun (i.e., $\vec{A} = A\widehat{Z} \| \widehat{S}$). This

[5] By constraining $\vec{A} \| \widehat{S}$, θ is minimized and P is maximized.

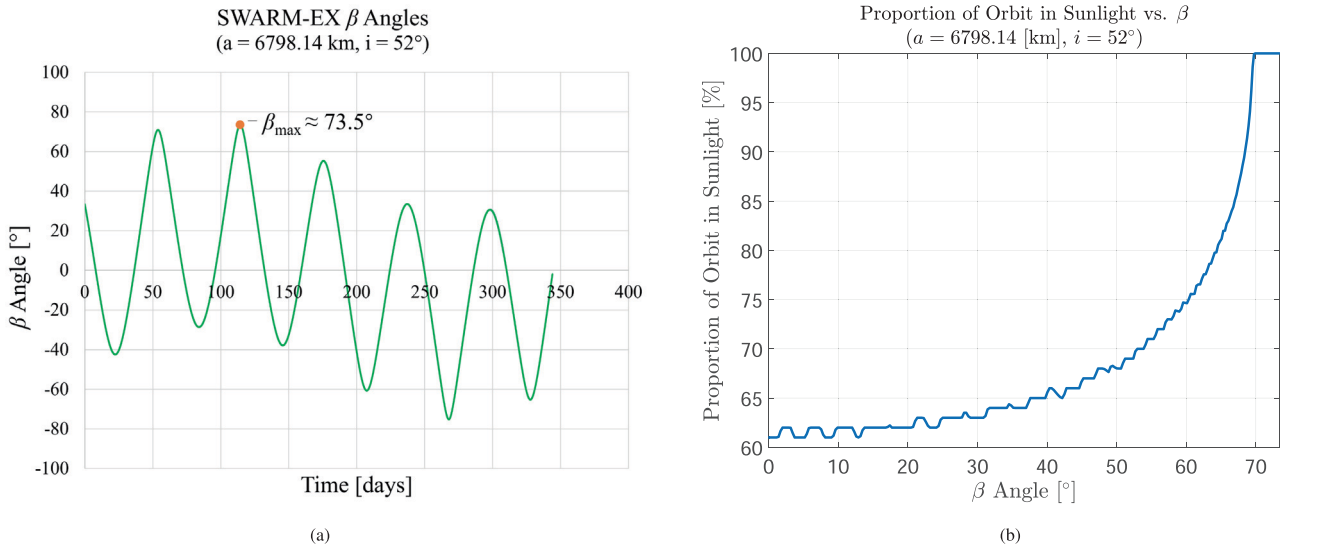

(a) (b)

Fig. 5. Characterization of β for the SWARM-EX mission in terms of (a) a year-long time series (with the peak value of $\beta_{max} \approx 73.5°$ annotated) and (b) the proportion of an orbit illuminated by the Sun as a function of β.

attitude is defined geometrically by the vector $\vec{\mathcal{L}}$ in Section 4 to which the instrument pointing vectors are aligned.[6]

3.1. β Angles

For a satellite in LEO, there will naturally be times when the Sun is obscured from the satellite by the Earth. The parameter commonly used to characterize this phenomenon is known as the β angle ($\beta \in [-90°, 90°]$), which is defined as the smaller angle between the satellite orbital plane and the satellite solar-ecliptic plane and serves as an indicator of the percentage of time that a satellite spends in direct sunlight (where it can absorb solar energy). Given that SWARM-EX is nominally due to launch from the International Space Station (ISS), the initial state vector $\mathbf{X}$ for the SWARM-EX mission is stated as

$$\begin{aligned}\mathbf{X}(t=0) &= (a_0, e_0, i_0, \Omega_0, \omega_0, M_0)^\intercal \\ &= (6798.14[\text{km}], 0.001, 52°, 45°, 90°, 0°)^\intercal \end{aligned} \quad (2)$$

for semi-major axis a, eccentricity e, inclination i, right ascension of the ascending node (RAAN) Ω, argument of periapsis ω, and mean anomaly M. As detailed by Fig. 5, these initial orbital state parameters produce a β which oscillates between sequential local minima and maxima with a period of around 30 days.[7] Given the symmetry that exists between positive and negative values of β which have the same magnitude vis-à-vis power generation, this work defines the minimum and maximum β angles for the SWARM-EX mission as $\beta_{min} = 0°$ and $\beta_{max} \approx 73.5°$, respectively.

Table 1
The dayside and nightside orbital proportions for both β_{min} and β_{max} orbits.

β [°]	Dayside	Nightside
0	62%	38%
≈73.5	100%	0%

Identifying the time-dependent nature of β illustrates two critical points regarding the SWARM-EX spacecraft power generation:

1. A singular orbit can be divided into the dayside (when the spacecraft is in the Sun) and the nightside (when the Earth obscures the Sun and the spacecraft is in eclipse). When $\beta = \beta_{max}$, the SWARM-EX spacecraft are never on the nighside. Table 1 and Fig. 5 define the dayside and nightside in terms of their orbital proportions for $\beta = \beta_{min}$ and $\beta = \beta_{max}$.
2. The SWARM-EX spacecraft will always have the potential to generate more power when $\beta = \beta_{max}$ compared to when $\beta = \beta_{min}$.[8]

While (2) is a consequence of (1), both distinctions are critical towards understanding the power generation capabilities of the SWARM-EX swarm in its particular orbit. As the duration of the dayside depends strongly on β, the subsequent power analysis analyzes the spacecraft power generation capabilities for both β_{min} and β_{max} to bound

[6] According to the spacecraft body frame detailed in Fig. 2, SCI experiments are characterized by $-\hat{Z} \| \vec{\mathcal{L}}$.

[7] The oscillation of β will change for different initial state vectors and is unique to the SWARM-EX orbit.

[8] β_{min} and β_{max} orbits are also commonly referred to as "noon-midnight" and "dawn-dusk orbits," respectively.

Table 2
Specifications for the STK CubeSat model file and the SWARM-EX spacecraft used to calculate the subsequent power values.

	P_{max} [W]	# Wing Cells	# Body Cells	# Wing Arrays	# Body Arrays
STK	1.03	7	7	2	1
SWARM-EX	1.18	7	5	4	1

the power problem between the worst-case and best-case power generation scenarios.

3.2. Simulating on-orbit power generation

The Systems Tool Kit (STK) by *Ansys* was chosen to simulate the on-orbit power generation of the SWARM-EX spacecraft (Ansys, 2024). Utilizing STK's internal Solar Panel Tool, which calculates the solar power P generated by the satellite model in use for a time duration specified by the user, the generated energy $\mathcal{P}$ and average power per orbit $\overline{P}$ are calculated as

$$\mathcal{P} = \overline{P} \cdot T = \left(\frac{1}{N}\sum_{j=1}^{N} P_j\right) \cdot T, \tag{3}$$

where P_j is the power at each time step index j and $N = \frac{T}{\Delta t}$ is the number of data points within an orbital period T for time step Δt.

As seen in Fig. 2, each SWARM-EX spacecraft will have four wing solar panels (i.e., those which are deployed at the beginning of the mission), each with seven solar cells, and one body-mounted solar panel (i.e., that which is mounted on the spacecraft body and does not deploy), with five solar cells.[9] Given that all solar panels and cells lie in the same plane, this configuration is denoted "Co-Planar 7–7-5-7–7." To circumvent the complex task of creating a 3D satellite object model compatible with STK[10], the pre-existing `cubesat_3u.dae` model is leveraged for this analysis. With a co-planar solar array configuration, this model bears a structural resemblance to the SWARM-EX spacecraft, which allows for its power-generation data to be mapped seamlessly to SWARM-EX (or any other satellite with a co-planar solar array configuration). Consequently, by incorporating the differences in solar cell type, solar cell peak power, and solar cell number between SWARM-EX and the STK satellite model, the power at each time step P_j can be found as

$$P_j = \left(\frac{P_{\max}}{P_{\max,\mathrm{STK}}}\right)\left(K_{\mathrm{wings}} P_{j,\mathrm{wings,STK}} + K_{\mathrm{body}} P_{j,\mathrm{body,STK}}\right), \tag{4}$$

where $P_{\max}, P_{j,\mathrm{wings}}$, and $P_{j,\mathrm{body}}$ are the peak power, power generated by the wing panels at index j, and power generated by the body-mounted panels at index j, respectively. The scale factor K is defined as

$$K = \left(\frac{\#\mathrm{cellsperpanel}}{\#\mathrm{cellsperpanelSTK}}\right)\left(\frac{\#\mathrm{panels}}{\#\mathrm{panelsSTK}}\right). \tag{5}$$

The parameters assumed into P_j are defined under AM0[11] conditions in Table 2 for SWARM-EX[12] and the pre-existing `cubesat_3u.dae` model in STK.

4. SCI Experiments: Constrained Attitude Profile

4.1. 100% Sun-Pointing and 100% Ram-Pointing

To illustrate the necessity of the constrained attitude profiles, the power generation capabilities of the best and worst case attitude profiles for power generation during SCI experiments are first highlighted. The attitude profile which maximizes power generation is denoted as "100% Sun-Pointing," or that attitude configuration which consistently maximizes power generation by constraining $\vec{A} \| \vec{S}$. When the methods of Section 3 are used to create a time series of the onboard power generated (Fig. 6), it can be shown that this attitude restriction eliminates all cosine power losses (i.e., $\theta(t) = 0°$). This attitude is most pertinent to the Safe Mode orbit timeline, to which a spacecraft will transition in the event that the battery SoC drops below a specified level (i.e., nominal operations are paused because the spacecraft needs to recharge). While optimal for power generation, 100% Sun-Pointing inhibits the spacecraft from consistently adhering to the other primary pointing restrictions, such as those imposed on the mission during SCI and GNC experiments. Maintaining the 100% Sun-Pointing attitude profile for an extended period of time is also expected to have significant thermal implications, potentially leading to overheating of the spacecraft and its onboard components.[13] If the objectives of the mission are to be accomplished, maximizing power at the expense of the other pointing requirements is prohibited. New attitudes must therefore be derived that optimize the balance

[9] As detailed in Section 4.5, the SWARM-EX power budget can be configured for additional solar panel/cell arrangements.
[10] A 3D satellite object model can be created in STK by importing a `.dae` file rendered in Collada from a `.stl` file or comparable 3D object file rendered in a Computer-Aided Design (CAD) software application.
[11] The standard spectrum outside the atmosphere is referred to as "AM0", meaning "zero atmospheres."
[12] SWARM-EX will use the Spectrolab XTE-SF solar cells (Spectrolab, 2024).
[13] Spacecraft thermal analysis extends beyond the scope of this work.

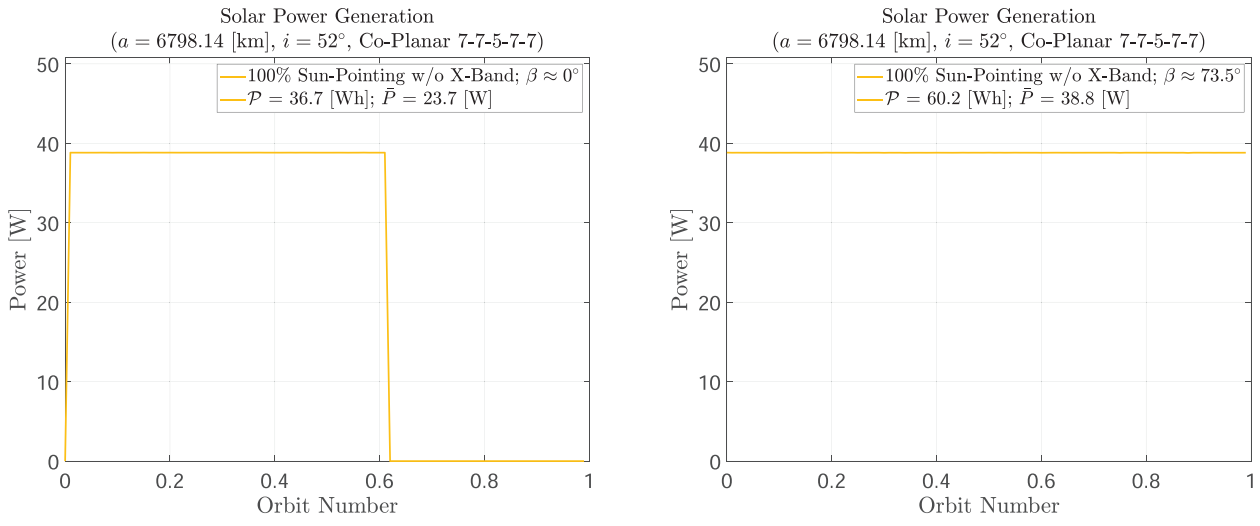

(a) $\beta = \beta_{\text{min}}$ (b) $\beta = \beta_{\text{max}}$

Fig. 6. The summation of the absorbed solar power for the SWARM-EX spacecraft in a Co-Planar 7–7-5-7–7 configuration at (a) $\beta = \beta_{\text{min}}$ and (b) $\beta = \beta_{\text{max}}$ over an entire orbit in the 100% Sun-Pointing attitude mode.

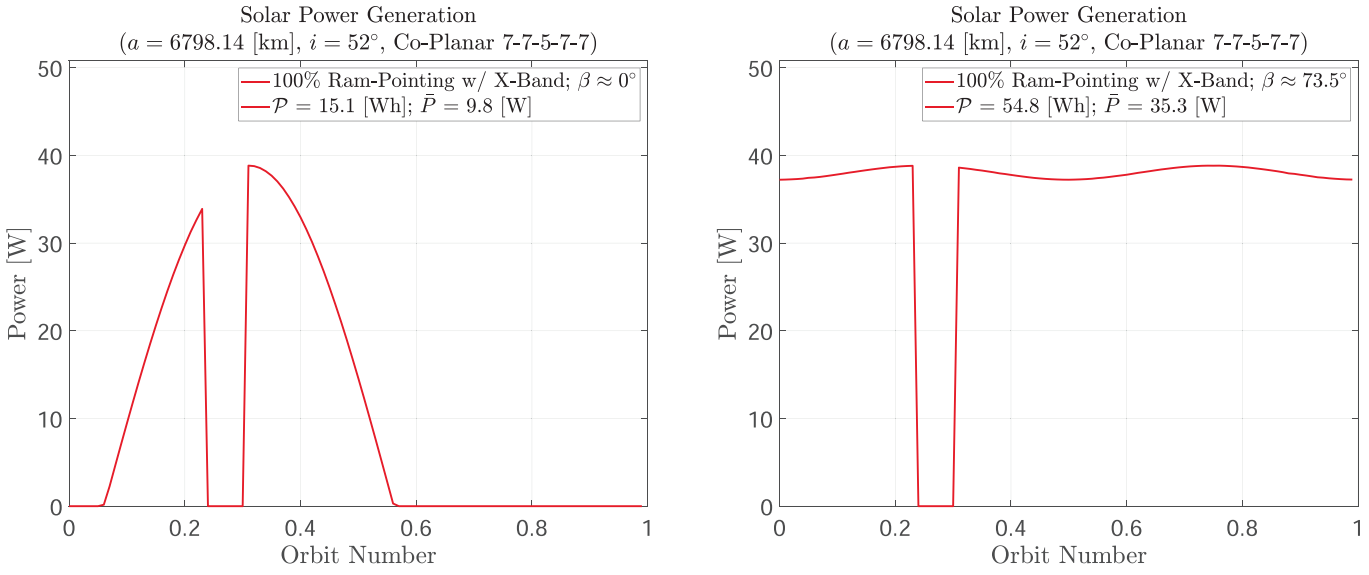

(a) $\beta = \beta_{\text{min}}$ (b) $\beta = \beta_{\text{max}}$

Fig. 7. The summation of the absorbed solar power for the SWARM-EX spacecraft in a Co-Planar 7–7-5-7–7 configuration at (a) $\beta = \beta_{\text{min}}$ and (b) $\beta = \beta_{\text{max}}$ over an entire orbit in the 100% Ram-Pointing attitude mode.

between power generation and all other mission constraints.

Next, "100% Ram-Pointing" is defined as the attitude profile which restricts the science instrument suite pointing vector to the ram-direction at all times and rolls the solar panels towards the Sun as much as possible without violating the ram constraint on the instruments. Moreover, the spacecraft are prescribed to also downlink on the X-Band when the ground station is visible. For a conservative estimate, it is assumed that the station location forces the spacecraft solar panels to rotate entirely away from the Sun, such that no power is generated during this 6% of the orbit.[14] 100% Ram-Pointing is the most trivial attitude configuration that satisfies the pointing requirements of the science instruments. However, although optimal for measurements by the FIPEX/LP, Fig. 7 reveals that when the solar panels are only given one degree of freedom (i.e., roll-

[14] Although the downlink period could occur anywhere in the orbit, the downlink period is located at the 24% mark of an orbit to align with the orbital timelines of Fig. 4. This decision yields a more conservative power estimate due to the overlap with FIPEX operations (0%-43%).

ing about the spacecraft body $\widehat{Z}$-axis), the inevitable power losses due to eclipse at $\beta_{\min}$ are supplemented by the significant cosine losses as the Sun passes overhead. Only when the Sun is directly overhead (i.e., $\theta = 0^\circ$) does $\vec{A} \| \vec{S}$ and power generation becomes maximized. The power losses are less significant at $\beta_{\max}$ because the Sun looms high in the sky relative to the spacecraft at these times (restricting θ) and there is no time spent on the nightside. Given that the least power draw from the orbital timelines relating to SCI is 15.9 [W] (Fig. 4), 100% Ram-Pointing will not allow the spacecraft to remain power positive during SCI experiments in $\beta_{\min}$ orbits when only 9.8 [W] is generated.

4.2. ψ-Cone off Ram

To circumvent the rigidity of the 100% Ram-Pointing profile, SWARM-EX mission designers have developed a novel constrained attitude profile which exploits the additional degree of freedom granted by the maximum angles allowed off ram for each instrument. The SWARM-EX science team has defined the maximum allowable angles off ram which still yield sufficient SNR as $\psi = 30^\circ$ for the FIPEX and $\lambda = 45^\circ$ for the LP. The preferred attitude configuration for SCI experiments is therefore one which constrains the spacecraft body $-\widehat{Z}$ pointing vector to a 30° or 45°-cone off ram while maximizing the time spent with the solar panel area vector parallel to the Sun pointing vector (i.e., $\vec{A} = -A\widehat{Y} \| \vec{S}$; Fig. 8).

In order to implement this attitude configuration in STK, a custom vector $\vec{\mathcal{L}}$ must first be defined for the satellite object in the SWARM-EX STK scenario via a `VBScript` plugin to which the spacecraft body $-\widehat{Z}$ vector must be aligned. The components of this custom vector $\vec{\mathcal{L}}$ are defined in reference to the Sun-Velocity angle $\angle SV$, the spacecraft velocity unit vector $\hat{v}$, and the Sun unit vector

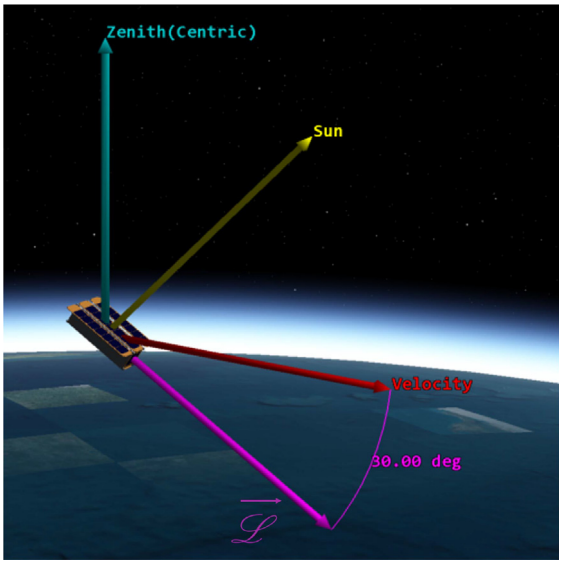

Fig. 8. A screenshot from STK illustrating the $\psi = 30^\circ$-Cone off Ram pointing mode in a $\beta_{\min}$ orbit.

$\widehat{S}$, all of which are defined and calculated by STK. Definition of the vector $\vec{\mathcal{L}}$ is then divided into four cases as a function of ψ or λ. For the analysis following this derivation, only ψ is used, as it is the more stringent requirement. Moreover, for the purposes of generality, the cases are defined in reference to an undefined $\psi \in [0^\circ, 90^\circ]$.[15]

The four cases illustrated by Fig. 9 are based on the following statements:

1. Define some vector of unknown magnitude $\vec{x} \| \widehat{S}$.
2. Let $\vec{\mathcal{L}} = \hat{v} + \vec{x} = \hat{v} - x\widehat{S}$.
3. Recall the Law of Sines: $\frac{\sin A}{a} = \frac{\sin B}{b}$ for some angles A and B of a triangle which face sides a and b, respectively.

With these definitions, all that must be done to define $\vec{\mathcal{L}}$ is to determine the value of x for each of the four cases. A.1 provides a verbose derivation of the custom vector $\vec{\mathcal{L}}$, which is shown to reflect the following piecewise function:

$$\vec{\mathcal{L}}\left(\psi, m\angle SV, \hat{v}, \widehat{S}\right) = \begin{cases} \hat{v} - \left[\frac{\sin\psi}{\sin(180^\circ - \psi - m\angle SV)}\right]\widehat{S}, & 0^\circ \leqslant m\angle SV < (90^\circ - \psi) \\ \hat{v} + [\sin(m\angle SV - 90^\circ)]\widehat{S}, & (90^\circ - \psi) \leqslant m\angle SV < (90^\circ + \psi) \\ \hat{v} + \left[\frac{\sin\psi}{\sin(m\angle SV - \psi)}\right]\widehat{S}, & (90^\circ + \psi) \leqslant m\angle SV < 180^\circ \end{cases} \tag{6}$$

With $\vec{\mathcal{L}}$ defined, there is additional logic that must be incorporated to complete the description of the primary attitude profile for SCI experiments. The first of these additions is to prevent the spacecraft from rolling over to catch the last minutes of sunlight as the Sun dips below the horizon. At small β angles (i.e., $\beta < 20^\circ$), this rolling is excessive, and it would not be feasible for the onboard ADCS to conduct 180° flips twice every orbit to catch this extra fragment of sunlight. Not only would this introduce unnecessary complexity to SWARM-EX operations, but it would also saturate the reaction wheels of the ADCS far too often, provoking a power spike that nearly negates the extra power generation altogether.[16] In order to implement this improvement, a second custom vector denoted $\vec{\mathcal{S}}$ to which the spacecraft body $-\widehat{Y}$ vector must be aligned while maintaining the ψ-cone off ram is defined to account for the times when $\beta < 20^\circ$ and the measure of the Sun-Zenith angle $\angle SZ$ is greater than $90^\circ - \psi$. At this point, $\vec{\mathcal{L}}$ is frozen in the spacecraft body frame and $\vec{\mathcal{S}}$ serves as a projection of $\widehat{S}$ rotated towards the zenith unit vector $\hat{z}$ by an angle of $90^\circ - \psi$ in the plane spanned by both $\hat{z}$ and $\widehat{S}$. Mathematically, this vector $\vec{\mathcal{S}}$ can be expressed as

$$\vec{\mathcal{S}}\left(\psi, m\angle SZ, \hat{z}, \widehat{S}\right) = \begin{cases} \widehat{S} + \left[\frac{\sin(m\angle SZ - 90^\circ + \psi)}{\sin(90^\circ - \psi)}\right]\hat{z}, & \beta < 20^\circ \text{and} m\angle SZ > (90^\circ - \psi) \\ \widehat{S}, & \text{else.} \end{cases} \tag{7}$$

[15] In the case where the FIPEX is turned off and only the LP pointing requirement remains, ψ can simply be replaced by λ.

[16] The power drawn by the ADCS during reaction wheel desaturation is modeled by the "ADCS Peak Power" in Fig. 3 and Fig. 11.

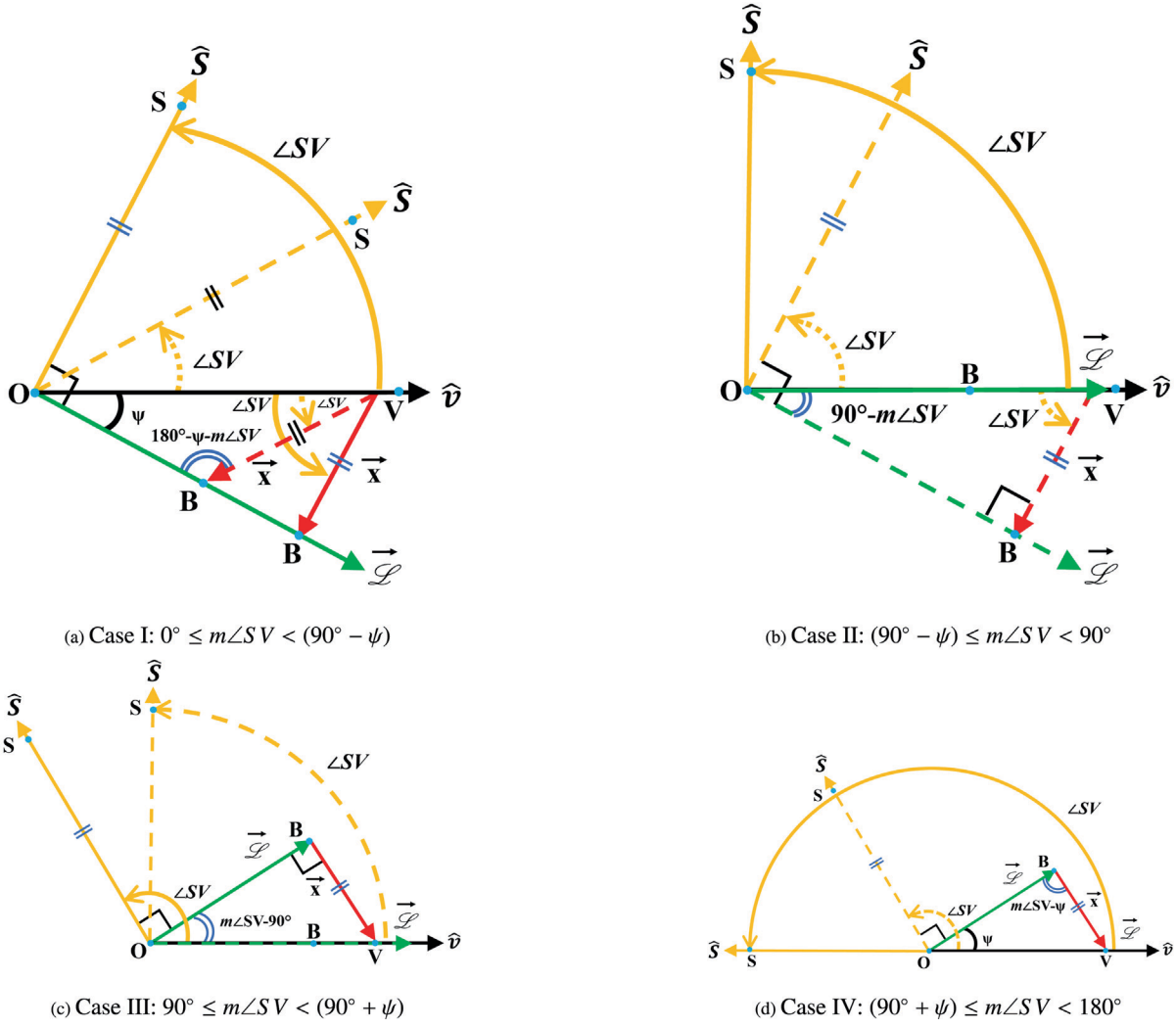

Fig. 9. Depictions of the geometry of $\vec{\mathcal{L}}$ for the (a) Case I: $0° \leqslant m\angle SV < (90° - \psi)$, (b) Case II: $(90° - \psi) \leqslant m\angle SV < 90°$, (c) Case III: $90° \leqslant m\angle SV < (90° + \psi)$, and (d) Case IV: $(90° + \psi) \leqslant m\angle SV < 180°$. The closed-face arrows represent vectors, and the open-faced arrows represent angles. The solid-lines and dashed-lines represent two separate groupings of equally probable scenarios within the case, with the dashed-lines indicating vector motion within the case.

Another improvement to this attitude profile is to align the spacecraft body $-\widehat{Z}$ with ram and the solar panel area vector with zenith (i.e., $\widehat{A} = \hat{z}$) when the spacecraft is on the nightside. Not only will this optimize measurements made by the LP (the FIPEX will not be operational on the nightside), but it will also ensure that the spacecraft GPS pointing vector is within 30° of zenith[17] to confidently receive at least one valid GPS update per orbit.[18] This requirement is imposed during SCI experiments to ensure sufficient Position, Navigation, and Timing (PNT) information for post-processing of the scientific instrument data. The PNT requirements mandated by GNC experiments and formation flying maneuvers are more stringent and extend beyond the scope of this study.

Finally, with the X-Band radio located on the spacecraft's body $+\widehat{Y}$-side, the attitude of the spacecraft during a downlink (denoted by $\epsilon > \epsilon_{\min}$ for elevation relative to the ground station ϵ) will be characterized by a ψ-cone off ram while maximizing the time the X-Band pointing vector is aligned with the ground station pointing vector. This attitude has an identical form to the previous solution of $\vec{\mathcal{L}}$, except with the Sun pointing vector $\widehat{S}$ replaced by the negative of the ground station pointing pointing vector $-\widehat{G}$ and $\angle SV$ replaced with $\angle GV$.

The improvements to the ψ-cone attitude profile produce the conditional paths defined in Algorithms 1 and 2.

[17] The farther off zenith the onboard GPS patch points, the fewer the number of GPS satellites in view, not to mention the less favorable geometries of the GPS constellations that arise (i.e., dilution of precision).

[18] While the spacecraft spend no time on the nightside in a $\beta_{\max}$ orbit, which would hinder their ability to roll towards zenith and confidently receive a valid GPS update, such an orbit rarely occurs and a non-zero eclipse time emerges as soon as $\beta \lessapprox 69°$. Moreover, even when rolled towards the Sun in a $\beta_{\max}$ orbit, the spacecraft are likely to still receive GPS updates. Thus, there is minimal concern regarding the validity of GPS updates during $\beta_{\max}$ orbits.

Algorithm 1. The logic used for $-\widehat{Z}$ alignment.

```
if nightside then
  if ϵ > ϵ_min then
    −Ẑ ← L⃗(ψ, m∠GV, v̂, −Ĝ)
  else
    −Ẑ ← v̂
  end if
else if dayside then
  if ϵ > ϵ_min then
    −Ẑ ← L⃗(ψ, m∠GV, v̂, −Ĝ)
  else
    −Ẑ ← L⃗(ψ, m∠SV, v̂, S⃗)
  end if
end if
```

Algorithm 2. The logic used for $-\widehat{Y}$ alignment.

```
if nightside then
  if ϵ > ϵ_min then
    −Ŷ ← −Ĝ
  else if
    then −Ŷ ← ẑ
  end if
  else if dayside then
  if ϵ > ϵ_min then
    −Ŷ ← −Ĝ
  else if
    −Ŷ ← S⃗
  end if
end if
```

With these new $\psi = 30°$-Cone and, by extension, $\lambda = 45°$-Cone attitude profiles defined, the solar panel cosine losses are mitigated significantly. As detailed by Fig. 10, the time that $\theta = 0°$ when $\beta = \beta_{\min}$ is increased from a single point in the 100% Ram-Pointing attitude to ≈20% of an orbit for the $\psi = 30°$-Cone attitude profile. **This allows the spacecraft to generate $> 62\%$ more power than when in the 100% Ram-Pointing attitude mode when $\beta = \beta_{\min}$.** Likewise, the flexibility of the $\psi = 30°$-Cone attitude profile **fully maximizes power generation when $\beta = \beta_{\max}$**, identical to the 100% Sun-Pointing configuration. These marked improvements are characterized in Table 3.

4.3. Mapping to Orbital Timelines

With the constrained attitude profile defined, mapping to the orbital timelines shown in Fig. 4 can be achieved by taking an aggregate of different attitude modes depending on the operational mode. For example, Table 4 details the breakdown for the "SCI Orbit w/ X-Band: Ground Station is Dayside" timeline, which contains various attitudes.

The "SCI Orbit w/ X-Band: Ground Station is Dayside" orbital timeline produces the greatest power draw of the timelines relating to SCI (i.e., 16.8 [W]; Table 4 and Fig. 4). If the 100% Ram-Pointing attitude profile was paired with this orbital timeline when $\beta = \beta_{\min}$, the 9.8 [W] generated (i.e., Fig. 7) would yield a net power of −7 [W]. However, when paired with the sequence of attitude profiles delineated by Table 4, the net power is + 2.6 [W]. This procedure can be applied to the other fourteen timelines in Fig. 4 to illustrate how the new constrained attitude profiles allow the spacecraft of SWARM-EX to remain power positive while still meeting the science pointing requirements regardless of β angle. This task is automated by the SWARM-EX Power Budget of Section 4.5 to fully characterize the spacecraft battery SoC.

4.4. Implications for Differential Drag

In order to minimize the amount of propulsion expended, SWARM-EX intends to utilize the appreciable orbital effects of atmospheric drag in LEO for maneuvers and formation reconfiguration. By altering the effective surface area perpendicular to the direction of motion of one of the spacecraft through a change in that spacecraft's attitude, the effects of atmospheric drag on spacecraft acceleration can be controlled. For a swarm of small satellites, management of spacecraft drag characteristics can be used to produce a difference in the acceleration between the spacecraft in the swarm. By tactfully implementing both Low-Drag (LD; minimum cross-sectional area) and High-Drag (HD; maximum cross-sectional area) attitude configurations, the acceleration difference due to drag known as "differential drag" will be used to vary the along-track separation between the CubeSats of SWARM-EX.

Increasing and decreasing the along-track separation between the SWARM-EX spacecraft (referred to as "expansion" and "contraction" of the swarm) is planned to occur during some of the mission's SCI experiments in an effort to evaluate the evolution of the EIA/ETA over varying spatial and temporal regions. Consequently, at least two of the three spacecraft in the swarm are required to maintain the ψ-Cone off Ram attitude profile during these differential drag maneuvers. For efficient expansion/-contraction, the SWARM-EX GNC team has identified that the differential inverse ballistic coefficient ΔB between the spacecraft must be at least 200%, where B and ΔB are defined as

$$B = \frac{C_D A_{\text{ref}}}{m}; \qquad \Delta B = \left| \frac{B_{\text{HD}} - B_{\text{LD}}}{B_{\text{LD}}} \right|, \tag{8}$$

where C_D is the drag coefficient, A_{ref} is the cross-sectional area, and m is the spacecraft mass.

Although the ψ-Cone and λ-Cone attitude configurations of Section 4 have been shown to facilitate a power-positive state, such profiles must also be manipulated to satisfy the additional constraint imposed by differential

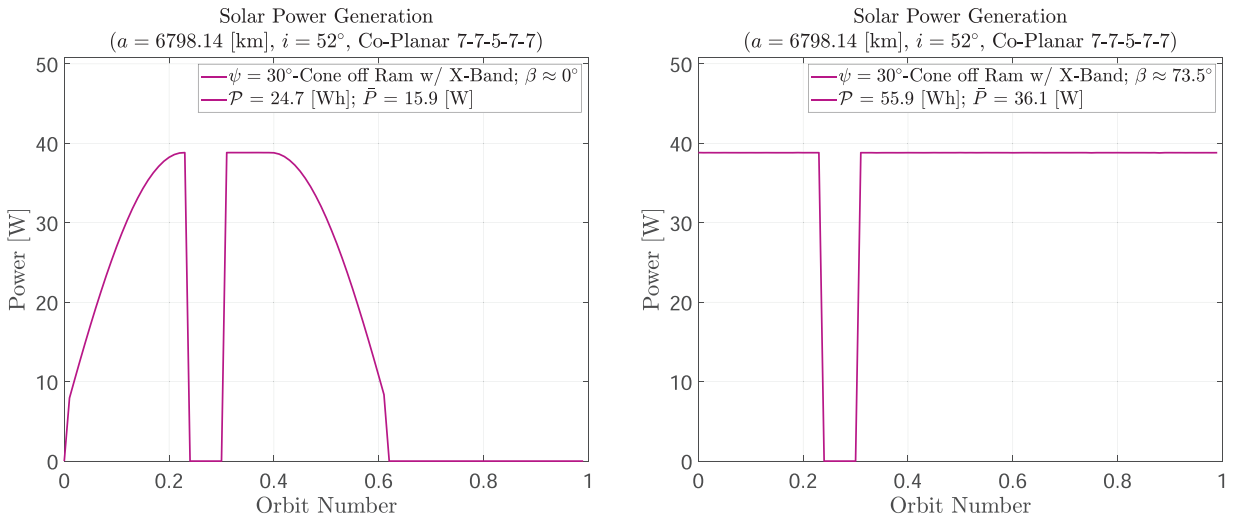

(a) $\beta = \beta_{\min}$ (b) $\beta = \beta_{\max}$

Fig. 10. The summation of the absorbed solar power for the SWARM-EX spacecraft in a Co-Planar 7–7-5-7–7 configuration w/ X-Band downlink at (a) $\beta = \beta_{\min}$ and (b) $\beta = \beta_{\max}$ over an entire orbit in the $\psi = 30°$-Cone attitude mode.

Table 3
The minimum and maximum values of $\bar{P}$ in [W] for the SWARM-EX spacecraft in a Co-Planar 7–7-5-7–7 configuration with X-Band downlink at $\beta = \beta_{\min}$ and $\beta = \beta_{\max}$ over an entire orbit in the 100% Ram-Pointing and $\psi = 30°$-Cone off Ram attitude modes alongside the power generation improvement from the 100% Ram-Pointing attitude profile to the $\psi = 30°$-Cone off Ram attitude profile.

β [°]	$\bar{P}_{\text{Ram}}$ [W]	$\bar{P}_{\text{SCI}}$ [W]	Improvement: Ram $\rightarrow \psi = 30°$
0	**9.8**	**15.9**	**62.2%**
≈73.5	**35.3**	**36.1**	**2.3%**

drag. For the one spacecraft where the science instrument suite is disabled, the SWARM-EX mission operators will impose the Safe Mode orbit timeline defined by the 100% Sun-Pointing attitude profile to produce the HD configuration. The other two satellites will be used to produce the LD configuration via one of the four science-based timelines of Fig. 4, which are characterized by amalgams of constrained attitude profiles (i.e., Section 4.3). Table 5 then illustrates that with these definitions, ΔB at both extremes of β is at least 200%, thereby indicating that the ψ-cone attitude profile also satisfies the requirements imposed by differential drag.[19] More advanced analyses which explore the effects of the constrained attitude profiles on satellite drag, such as assessing their influence on the aerodynamic force coefficients or delving into formation flying control theory, extend beyond the purview of this study.

4.5. SWARM-EX Power Budget: A Spacecraft Battery State of Charge Simulation Tool

The derivation of the constrained attitude profiles of Section 4 allows the SWARM-EX mission designers to define each of the fifteen orbital timelines of Fig. 4 as a sequence of operational modes paired with a progression of attitude configurations. To facilitate the procedure of Section 4.3 for the other fourteen timelines, mission designers have developed the SWARM-EX Power Budget, an automated, user-interactive Microsoft Excel spreadsheet[20] which simulates the battery SoC for three orbital timelines and parameters of the user's choosing (Fig. 11). Configurable items include the simulated orbital timelines, β angle, solar panel/cell configuration, solar cell specifications (i.e., peak power, efficiency, yearly degradation, temperature gradients), and battery capacity [Wh]. Following the definitions of these parameters, the power budget takes in the power draw and power generated at each time step (1% of an orbit) to calculate the corresponding battery SoC $\in [0\%, 100\%]$ as

$$\text{SoC} = \frac{\mathcal{P}_{\text{generated}} - \mathcal{P}_{\text{used}}}{\mathcal{P}_{\text{max,battery}}} \times 100\%. \tag{9}$$

Eq. (9) reveals that if $\mathcal{P}_{\text{used}} > \mathcal{P}_{\text{generated}}$, the SoC drops below 100% and the spacecraft is forced to draw energy from the battery. While this phenomenon is expected, if the SoC continues to decrease without check, the spacecraft batteries will deplete and the spacecraft will become inoperable. As detailed by Section 4.3, all timelines must be designed to yield a net positive return from a weighted

[19] Throughout an expansion/contraction, the satellites in the swarm will be re-tasked as either LD or HD according to the desired final swarm configuration. Each expansion/contraction is estimated to span a month-long period.

[20] The choice to design the power budget in Excel was made because Excel is a prevalent application with a reduced learning curve for students with minimal skills in computer programming.

Table 4
The operational modes, duty cycles, attitude profiles, and power specifications for the "SCI Orbit w/ X-Band: Ground Station is Dayside" orbital timeline.

Mode	Duty Cycle	Attitude Profile	Draw [W]	Generated [W]
FPX1	24%	$\psi = 30°$-Cone off Ram; Maximize Sun-Pointing	4.6	6.4
FPX3	6%	$\psi = 30°$-Cone off Ram; Maximize Ground-Pointing	3.0	0.6
FPX1	13%	$\psi = 30°$-Cone off Ram; Maximize Sun-Pointing	2.5	5.0
SP1	56%	$\lambda = 45°$-Cone off Ram; Maximize Sun-Pointing	6.5	7.4
PROP OPS	1%	100% Ram-Pointing	0.2	0.0
		Totals:	16.8	19.4
		Net:	**+ 2.6**	

Table 5
Average ΔB over an orbital period at β_{min} and β_{max} during the differential drag expansions/contractions of SWARM-EX.

	β_{min}		β_{max}	
	Low Drag	**High Drag**	**Low Drag**	**High Drag**
Operational Orbit:	SCI	Safe Mode	SCI	Safe Mode
Average ΔB:	354.3%		200%	

average energy-in energy-out calculation (i.e., Table 4) for a spacecraft to remain power positive. However, a more precise indicator for power stability is the ability of the SoC to return to 100% after a few orbits. For this reason, the focal point of the power budget is a time series of the SoC following three full orbits and a calculation of time until battery depletion based on the slope of the SoC (if possible). If the batteries are unable to recharge to full capacity within three orbits, the sequence is deemed unstable. The selection of three orbits as the benchmark for power stability is aligned with the risk profile established by the SWARM-EX mission designers. This parameter is adaptable and can be modified based on preference.

Serving as the culmination of the power analysis, the power budget indicates that **the SWARM-EX spacecraft will remain power-positive during all fifteen orbital timelines**. This not only validates the efficacy of the constrained attitude profiles of Section 4, but it also concisely assures the team that the mission is well-positioned for success from the perspective of power.[21]

5. Conclusion

While the CubeSat standard generates many advantages, the structural rigidity and size limitations which accompany the design often manifest challenges for mission designers from the perspective of power. Seeking to concurrently investigate equatorial space weather phenomena and advance the state-of-the-art in spacecraft swarming, the Space Weather Atmospheric Reconfigurable Multiscale-EXperiment (SWARM-EX) CubeSat mission is a paragon of this reality. With numerous pointing and power requirements imposed by the onboard science instrument suite, radios, and other subsystems, satisfying all these constraints and the objectives of the mission demands prudent design choices for a CubeSat with limited power-generation capabilities and attitude freedom.

Acknowledging the complexity of the mission's technical objectives, the SWARM-EX mission designers have developed a process for analyzing a spacecraft's on-orbit power stability that combines a Concept of Operations (ConOps) constructed from operational modes and orbital timelines, constrained attitude profiles simulated in the Systems Tool Kit (STK) by *Ansys*, and an automated State of Charge (SoC) simulation tool, which serves as the mission's power budget. The module-based approach to the ConOps classifies all possible on-orbit power-draw states based on projected mission operations for the SWARM-EX mission. The attitude profiles developed are derived geometrically to satisfy the various pointing requirements during science experiments while simultaneously maximizing power generation. When these profiles are applied to the SWARM-EX orbit, the intersection of the ConOps with the power values generated by STK in these attitude profiles allows the power budget to readily illuminate critical power issues, thereby facilitating improved comprehension of spacecraft performance during each mission phase.

As small satellite projects continue to push scientific and technical boundaries, coordinated processes like these will become more necessary for successful operations. The approach described here has allowed the SWARM-EX mission designers to systematically mitigate the risk of not sustaining power-positive operations; the team is now confident that the spacecraft swarm will have enough power to execute the mission's objectives. While the methodologies outlined here are tailored to address the specific needs of the SWARM-EX mission, the authors aim to have these techniques serve as a specific case from which more advanced planning processes can be derived, some of which may proliferate to other small satellite projects throughout the field. The framework presented here for carefully analyzing power stability, developing constrained attitude profiles, and implementing a module-based ConOps is versatile and lends itself to adaptation for integration into diverse small satellite endeavors. Such

[21] Because the SWARM-EX power budget contains proprietary and export-controlled information, it cannot be shared publicly. However, the authors are amenable to being contacted with questions/advice regarding the tool.

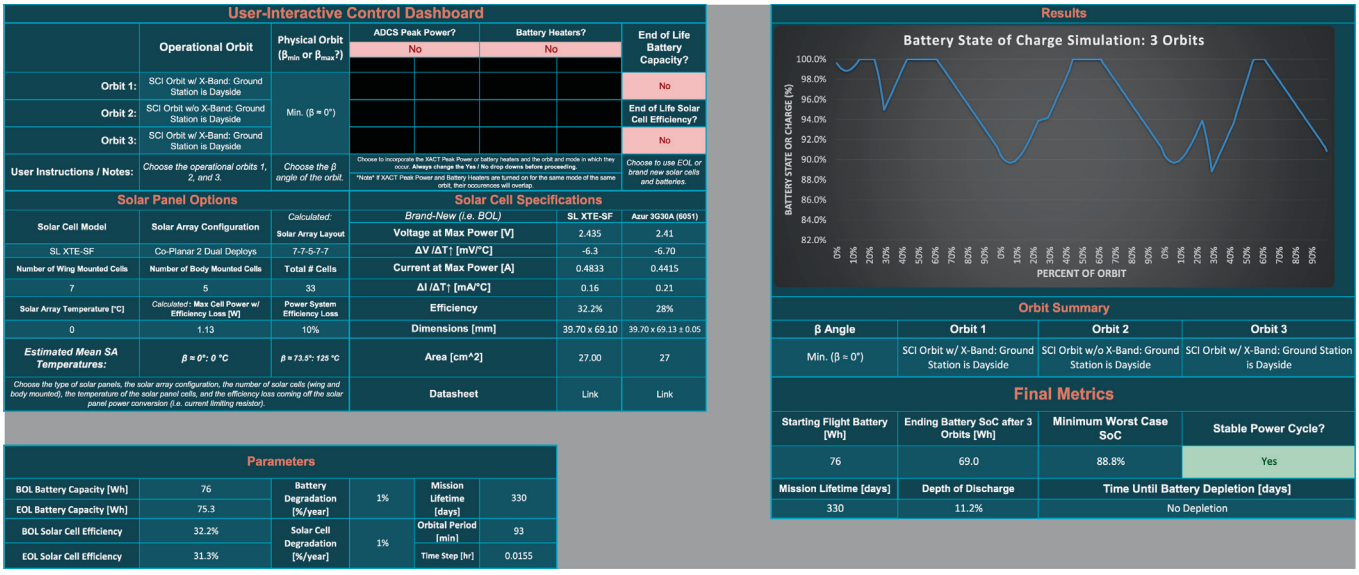

Fig. 11. A screenshot from the SWARM-EX power budget illustrating its capability to simulate the battery SoC for three orbital timelines (three SCI orbits at $\beta = \beta_{\min}$ are shown) of the user's choosing, allow the input of various parameters, and identify the stability of the spacecraft power state.

adaptability extends its utility beyond the confines of a singular mission, providing valuable insights for managing power constraints and enhancing satellite performance across a variety of mission objectives. By embracing this holistic approach, future missions can navigate the complexities of space exploration with confidence and precision, driving progress and discovery in the realm of small satellite technology.

Declaration of Competing Interest

The authors declare that they have no known competing financial interests or personal relationships that could have appeared to influence the work reported in this paper.

Acknowledgments

This work was supported by the National Science Foundation (award numbers: 1936512, 1936518, 1936537, 1936538, 1936550, 1936665). The authors would also like to particularly acknowledge Evan Bauch[22] and Rohil Agarwal[23] for their contributions.

Appendix A. ψ-Cone Verbose Derivation

A.1. ψ-Cone Verbose Derivation

This subsection details a verbose derivation of the four cases detailed by Fig. 9 for $\vec{\mathcal{L}}$.

A.1.1. Case I: $0^\circ \leqslant m\angle SV < (90^\circ - \psi)$

In this case, due to the relationship between $\angle SV$ and ψ, the constraint to maximize solar power generation makes the ψ-cone the limiting factor, such that the spacecraft is locked into an attitude configuration that is $-\psi^\circ$ off ram and yields non-optimal solar power generation according to the value of $\theta = 90^\circ - \angle BOS$, the angle between $\vec{\mathcal{L}}$ and $\widehat{S}$. Then, according to the Law of Sines,

$$\frac{\sin\psi}{x_{\mathrm{I}}} = \frac{\sin\left(180^\circ - \psi - m\angle SV\right)}{|\hat{v}|} = \sin\left(180^\circ - \psi - m\angle SV\right), \tag{A.1}$$

where the fact that the magnitude of a unit vector such as $|\hat{v}| = 1$ has been used. x_{I} can then be solved for and, subsequently, $\vec{\mathcal{L}} = \vec{\mathcal{L}}_{\mathrm{I}}$ as

$$\vec{\mathcal{L}}_{\mathrm{I}} = \hat{v} - x_{\mathrm{I}}\widehat{S} = \hat{v} - \left[\frac{\sin\psi}{\sin\left(180^\circ - \psi - m\angle SV\right)}\right]\widehat{S}. \tag{A.2}$$

A.1.2. Case II: $(90^\circ - \psi) \leqslant m\angle SV < 90^\circ$

The relationship between $\angle SV$ and ψ in this case allows the spacecraft to remain within the ψ-cone off ram while maximizing solar panel power generation (i.e., $\theta = 0^\circ$) always. Depending on the location of the Sun, the spacecraft will rotate through $-\psi^\circ$ off ram to 0° off ram (i.e., $\vec{\mathcal{L}} \| \hat{v}$). From this configuration, the Law of Sines produces

$$\frac{\sin\left(90^\circ - m\angle SV\right)}{x_{\mathrm{II}}} = \frac{\sin\left(90^\circ\right)}{|\hat{v}|} = 1. \tag{A.3}$$

x_{II} can then be solved for and, subsequently, $\vec{\mathcal{L}} = \vec{\mathcal{L}}_{\mathrm{II}}$ as

$$\vec{\mathcal{L}}_{\mathrm{II}} = \hat{v} - x_{\mathrm{II}}\widehat{S} = \hat{v} - \left[\sin\left(90^\circ - m\angle SV\right)\right]\widehat{S}. \tag{A.4}$$

[22] Laboratory for Atmospheric and Space Physics, University of Colorado, Boulder, 1234 Innovation Drive, Boulder, CO 80303

[23] Zipline, 333 Corey Way, South San Francisco, CA 94080

A.1.3. Case III: $90^\circ \leqslant m\angle SV < (90^\circ + \psi)$

Case III is the counterpart to Case II, in that the relationship between $\angle SV$ and ψ allows the spacecraft to remain within the ψ-cone off ram while maximizing solar panel power generation (i.e., $\theta = 0^\circ$) always. Depending on the location of the Sun, the spacecraft will rotate through 0° off ram (i.e., $\vec{\mathcal{L}} \| \hat{v}$) to $+\psi^\circ$ off ram. From this configuration, the Law of Sines produces

$$\frac{\sin(m\angle SV - 90^\circ)}{x_{\mathrm{III}}} = \frac{\sin(90^\circ)}{|\hat{v}|} = 1. \tag{A.5}$$

x_{III} can then be solved for and, subsequently, $\vec{\mathcal{L}} = \vec{\mathcal{L}}_{\mathrm{III}}$ as

$$\vec{\mathcal{L}}_{\mathrm{III}} = \hat{v} - x_{\mathrm{III}}\widehat{S} = \hat{v} - [\sin(m\angle SV - 90^\circ)]\widehat{S}. \tag{A.6}$$

By comparing Eq. (A.4) and (A.6), it can be seen that $\vec{\mathcal{L}}_{\mathrm{II}} = \vec{\mathcal{L}}_{\mathrm{III}}$, indicating that $\vec{\mathcal{L}}$ has identical solutions for the period of time when the spacecraft rotates through the ψ-cone (i.e., from $-\psi^\circ$ to $+\psi^\circ$) to track the Sun.

A.1.4. Case IV: $(90^\circ + \psi) \leqslant m\angle SV < 180^\circ$

The final case, Case IV, is the counterpart to Case I, as the constraint to maximize solar power generation once again makes the ψ-cone the limiting factor. The spacecraft is locked into an attitude configuration that is $+\psi^\circ$ off ram and yields non-optimal solar power generation according to the value of $\theta = 90^\circ - \angle BOS$. Then, according to the Law of Sines,

$$\frac{\sin\psi}{x_{\mathrm{IV}}} = \frac{\sin(m\angle SV - \psi)}{|\hat{v}|} = \sin(m\angle SV - \psi). \tag{A.7}$$

x_{IV} can then be solved for and, subsequently, $\vec{\mathcal{L}} = \vec{\mathcal{L}}_{\mathrm{IV}}$ as

$$\vec{\mathcal{L}}_{\mathrm{IV}} = \hat{v} - x_{\mathrm{IV}}\widehat{S} = \hat{v} - \left[\frac{\sin\psi}{\sin(m\angle SV - \psi)}\right]\widehat{S} \tag{A.8}$$

Appendix B. Acronyms

ADCS	Attitude Determination Control System
AM0	Zero Atmospheres
CAD	Computer-Aided Design
CDH	Command & Data Handling
ConOps	Concept of Operations
CSSWE	Colorado Student Space Weather Experiment
CU	University of Colorado
DD	Differential Drag
EIA	Equatorial Ionization Anomaly
ETA	Equatorial Thermospheric Anomaly
EPS	Electrical Power System
FIPEX	Flux Probe EXperiment
GNC	Guidance Navigation & Control
GPS	Global Positioning System
HD	High-Drag
ISS	International Space Station
km	Kilometer
LASP	Laboratory for Atmospheric and Space Physics
LD	Low-Drag
LEO	Low-Earth Orbit
LP	Langmuir Probe
MinXSS	Miniature X-ray Solar Spectrometer
NSF	National Science Foundation
PNT	Position, Navigation, and Timing
PROP	Propulsion
RAAN	Right Ascension of the Ascending Node
SCI	Science
SNR	Signal-to-Noise Ratio
SoC	State of Charge
STK	Systems Tool Kit
SWARM-EX	Space Weather Atmospheric Reconfigurable Multiscale-EXperiment
UHF	Ultra-High Frequency
VBScript	VisualBasic Script
w/	with
W	Watts
Wh	Watt-Hours

Appendix C. Symbols

a	Semimajor axis
A_{ref}	Cross-sectional area
$\vec{A}$	Solar panel area pointing vector
B	Inverse ballistic coefficient
ΔB	Differential inverse ballistic coefficient
β	Beta angle
β_{min}	Minimum beta angle
β_{max}	Maximum beta angle
C_{D}	Drag coefficient
e	Eccentricity
η	Solar panel efficiency
ϵ	Elevation relative to the ground station
ϵ_{min}	Minimum allowable elevation relative to the ground station to downlink
$\vec{G}$	Ground station pointing vector
$\angle SV$	Ground Station-Velocity angle
$\angle GZ$	Ground Station-Zenith angle
i	Inclination
j	Time step index
$\vec{\mathcal{J}}$	Solar panel flux vector
K	Satellite object model scale factor
$\vec{\mathcal{L}}$	Custom vector used for attitude during SCI experiments
λ	Maximum angle allowed off ram when the Langmuir Probe is operational
m	Mass
M	Mean anomaly
Ω	Right ascension of the ascending node (RAAN)
ω	Argument of periapsis

(continued on next page)

$\mathcal{P}$	Energy [Wh]
P	Power [W]
$\overline{P}$	Average power per orbit [W]
ψ	Maximum angle allowed off ram when the FIPEX is operational
$\vec{S}$	Sun vector originating at the spacecraft
$\vec{\mathcal{S}}$	Constrained Sun vector
$\angle SV$	Sun-Velocity angle
$\angle SZ$	Sun-Zenith angle
t	Time
T	Orbital period
Δt	Time step
θ	Angle between $\vec{S}$ and $\vec{A}$
$\hat{v}$	Velocity unit vector
$\mathbf{X}$	Spacecraft State Vector
$\widehat{X}$	Spacecraft body pointing vector
$\widehat{Y}$	Spacecraft body pointing vector
$\vec{z}$	Zenith (Centric) vector
$\widehat{Z}$	Spacecraft body pointing vector

References

Ansys, 2024. Ansys stk: Software for digital mission engineering and systems analysis. URL: https://www.ansys.com/products/missions/ansys-stkretrieved2024-05-17.

Appleton, S., 1946. Two anomalies in the ionosphere. Nature 71 (3995), 3995-3995.

Eberhart, M., Löhle, S., Steinbeck, A., et al., 2015. Measurement of atomic oxygen in the middle atmosphere using solid electrolyte sensors and catalytic probes. Atmos. Meas. Tech. 8 (9), 3701–3714.

Fish, C., Swenson, C., Crowley, G., et al., 2014. Design, development, implementation, and on-orbit performance of the dynamic ionosphere cubesat experiment mission. Space Sci. Rev. 181 (1–4), 61–120. https://doi.org/10.1007/s11214-014-0034-x.

Hunter, M., D'Amico, S., 2022. Closed-form optimal solutions for propulsive-differential drag control of spacecraft swarms. In: Proceedings of the AAS/AIAA Astrodynamics Specialist Conference.

Li, X., Schiller, Q., Blum, L. et al., 2013. First results from csswe cubesat: Characteristics of relativistic electrons in the near-earth environment during the october 2012 magnetic storms. J. Geophys. Res.: Space Phys., 118(10), 6489–6499. URL: https://agupubs.onlinelibrary.wiley.com/doi/abs/10.1002/2013JA019342. doi: 10.1002/2013JA019342. arXiv:https://agupubs.onlinelibrary.wiley.com/doi/pdf/10.1002/2013JA019342.

Liu, H., Lühr, H., Watanabe, S., 2007. Climatology of the equatorial thermospheric mass density anomaly. J. Geophys. Res.: Space Phys., 112(A5). URL: https://agupubs.onlinelibrary.wiley.com/doi/abs/10.1029/2006JA012199. doi: 10.1029/2006JA012199. arXiv:https://agupubs.onlinelibrary.wiley.com/doi/pdf/10.1029/2006JA012199.

Lowe, S., Fitzpatrick, D., Buynovskiy, A., et al., 2024. Concept of operations for swarm-ex: a three cubesat formation-flying mission [manuscript submitted for publication]. In: Proceedings of the IEEE Aerospace Conference.

Marshall, M.A., Goel, A., Pellegrino, S., 2020. Power-optimal guidance for planar space solar power satellites. J. Guidance, Control, Dynam., 43(3), 518–535. URL: doi: 10.2514/1.G004643. doi:10.2514/1.G004643. arXiv:https://doi.org/10.2514/1.G004643.

Palo, S.E., Rainville, N., Dahir, A., et al., 2015. One of 50: Challenger, the University of Colorado Boulder QB50 Constellation Satellite. In: In AGU Fall Meeting Abstracts, pp. A53A–0359, volume 2015.

Porras-Hermoso, A., Marín-Coca, S., González-Monge, J., et al., 2024. Derivation of a sun-tracking law for payloads with pointing restrictions in the upmsat-3 mission. J. Phys: Conf. Ser. 2716 (1), 012098. https://doi.org/10.1088/1742-6596/2716/1/012098.

Puig-Suari, J., Turner, C., Ahlgren, W., (2001). Development of the standard cubesat deployer and a cubesat class picosatellite. In: 2001 IEEE Aerospace Conference Proceedings (Cat. No.01TH8542) (pp. 1/347–1/353 vol 1). volume 1. doi:10.1109/AERO.2001.931726.

Spectrolab (2024). Xte-sf (standard fluence): Space qualified triple junction solar cell datasheet. URL: https://www.spectrolab.com/photovoltaics/XTE-SF_Data_Sheet.pdf retrieved 2024-05-17.

Woods, T.N., Caspi, A., Chamberlin, P.C., et al., 2016. Mission Overview of the Miniature X-ray Solar Spectrometer (MinXSS) CubeSat. In AAS/Solar Physics Division Abstracts #47. In: volume 47 of AAS/Solar Physics Division Meeting, p. (p. 8.16)..